NMR Spectroscopy

What you get . . .

depends on where you look

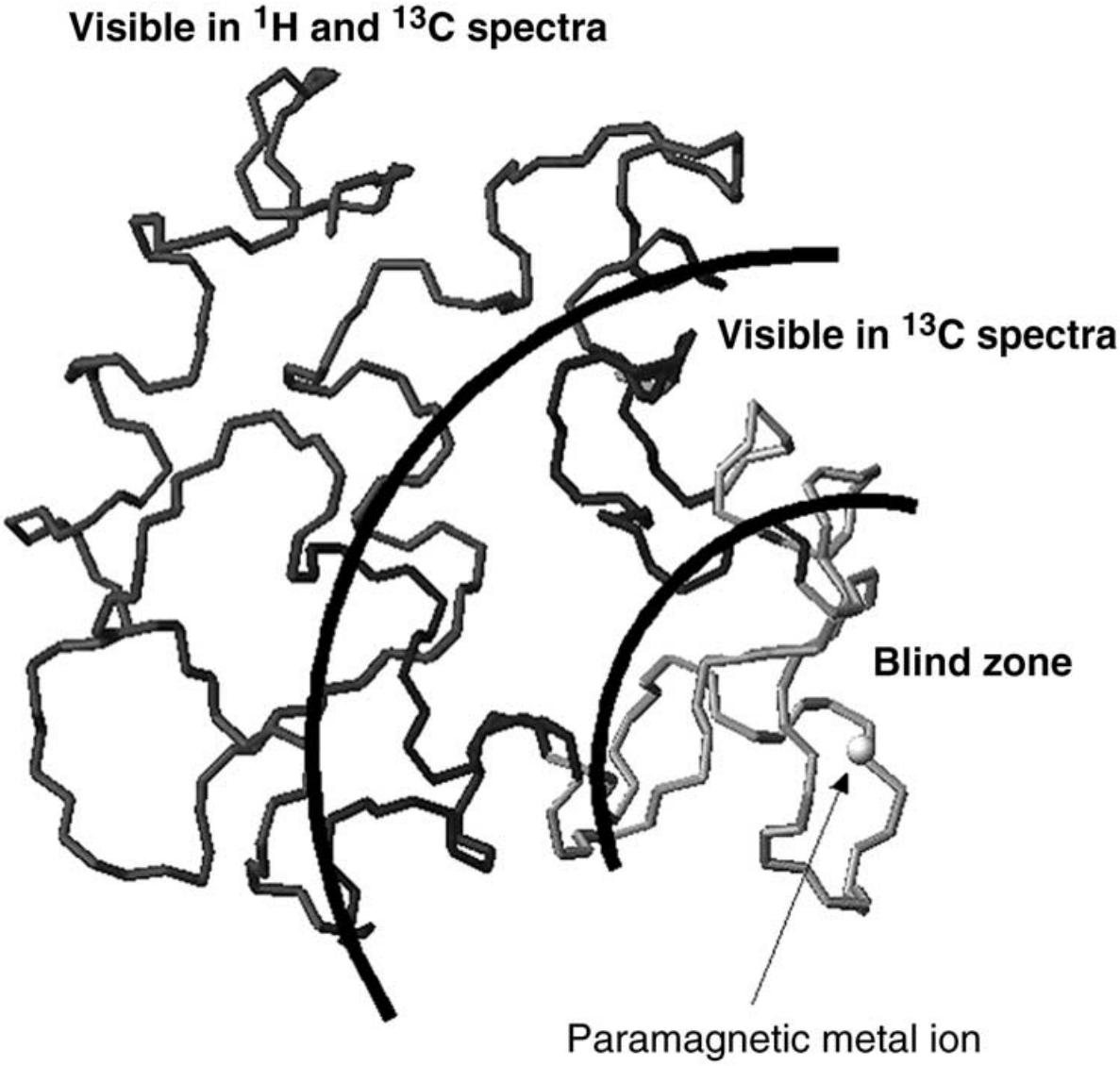

  DOI: 10.1002/cbic.200500124 *ChemBioChem* **2005**, *6*, 1536 – 1549

NMR Spectroscopy of Paramagnetic Metalloproteins

Ivano Bertini,*[a, b] Claudio Luchinat,[a, c] Giacomo Parigi,[a, c] and Roberta Pierattelli[a, b]

This article deals with the solution structure determination of paramagnetic metalloproteins by NMR spectroscopy. These proteins were believed not to be suitable for NMR investigations for structure determination until a decade ago, but eventually novel experiments and software protocols were developed, with the aim of making the approach suitable for the goal and as user-friendly and safe as possible. In the article, we also give hints for the optimization of experiments with respect to each particular metal ion, with the aim of also providing a handy tool for non-specialists. Finally, a section is dedicated to the significant progress made on ^{13}C direct detection, which reduces the negative effects of paramagnetism and may constitute a new chapter in the whole field of NMR spectroscopy.

1. Introduction

From genome browsing, it appears that the number of known proteins that need a metal ion to function is increasing more and more. It is estimated that about $^1/_4$ of the proteins in all living organisms contain a metal ion.[1] In the human genome alone, about 10% of the total are proteins that require zinc. Calcium, iron, and copper are also abundant and essential metal cofactors.

If we look at metalloproteins by NMR spectroscopy, the metal ion represents a point of discontinuity in the network of coherence transfer and in the structural restraints. Therefore, metalloproteins represent a challenge from the point of view of solution structure determination by NMR spectroscopy.

Indeed, there are many NMR-derived structures of metalloproteins deposited in the Protein DataBank,[2] but often the ligands and the atoms coordinated to the metal ion are assumed to be known by analogy with X-ray structures of homologous proteins and the coordination bonds are imposed as restraints. In some lucky cases, metal-nucleus–proton scalar connectivities can be exploited to prove the existence of a metal–protein bond. This is the case with ^{113}Cd[3–6] and ^{199}Hg,[7,8] for which metal–ligand couplings can be detected by heteronuclear 2D experiments such as metal–proton correlation or metal-edited spectra. These experiments provide cross-peaks originating from the metal-nucleus–proton couplings, which are directly related to the MXCH dihedral angle (M = metal ion; X = donor atom; Figure 1).[9] In this way, structure information on the coordination geometry of the metal site can be obtained. Such measurements are possible, although in the case of metal nuclei with $I > ^1/_2$ quadrupolar relaxation may easily broaden the lines, with the result that the connectivity is quenched. Our group has pursued the use of X-ray absorption spectroscopy (XANES, edge, and EXAFS) to obtain information on the number and nature of donor atoms and their distance from the metal ion.[10,11] The cysteine/methionine and histidine ligands are easily detected as donor groups.[12,13]

Among metalloproteins, paramagnetic metalloproteins represent a chapter by themselves. They are characterized by the presence of unpaired electrons. Therefore, EPR and ENDOR spectroscopy are complementary information tools to NMR spectroscopy.[14,15] Unpaired electrons have large magnetic moments (the free electron has a magnetic moment 658 times

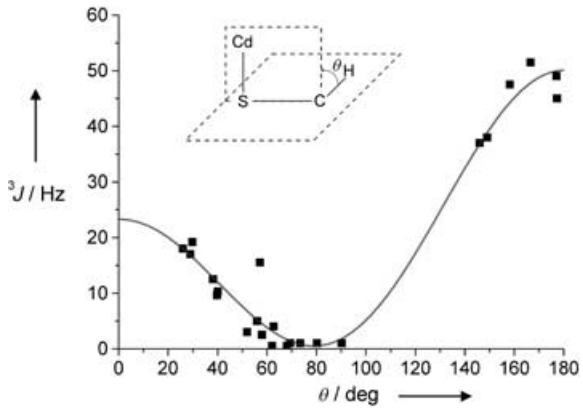

Figure 1. Karplus-type relationship between the $^{113}Cd–S–C–H$ dihedral angle, θ, and the metal–proton coupling constant, ^3J, in Cd_7-metallothionein and Cd-rubredoxin, with the best-fit curve shown.[9]

[a] *Prof. I. Bertini, Prof. C. Luchinat, Dr. G. Parigi, Prof. R. Pierattelli*
Magnetic Resonance Center, University of Florence
Via Luigi Sacconi 6, 50019 Sesto Fiorentino (Italy)
Fax: (+39) 055-457-4271
E-mail: ivanobertini@cerm.unifi.it

[b] *Prof. I. Bertini, Prof. R. Pierattelli*
Department of Chemistry, University of Florence
Via della Lastruccia 6, 50019 Sesto Fiorentino (Italy)

[c] *Prof. C. Luchinat, Dr. G. Parigi*
Department of Agricultural Biotechnology, University of Florence
Via Gaetano Donizetti 6, 50144 Florence (Italy)

 DOI: 10.1002/cbic.200500124

larger than a proton) and have relaxation times varying from 10^{-13}–10^{-8} s depending on the atomic number of the metal and on the particular occupancy of the atomic orbitals. Electron relaxation generates stochastic magnetic fields which cause nuclear relaxation.[16,17]

The understanding of electron relaxation and its effect on nuclear relaxation is another challenging field of research, which is pertinent to NMR spectroscopy of paramagnetic molecules because the resulting nuclear relaxation properties determine the observability of NMR spectra.

Although some approximation is necessary, we can say that in the presence of paramagnetic metal ions the NMR lines broaden with the reciprocal of the 6th power of the metal–nucleus distance.[18–21] Therefore, generally there is a sphere around the metal ion in which proton NMR lines are too broad to be detected, a shell in which nuclei give rise to observable but broad lines, and a further shell in which the paramagnetic effect is negligible (Figure 2). The size of these shells depend on the nuclear relaxing capability of the metal ion, which in turn depends on the number of unpaired electrons, on the electron relaxation time, and on the rotational correlation time of the molecule (see Section 2.2). The nuclear relaxing capability of various metal ions for a protein of a given size are summarized in graphical form in Figure 3.

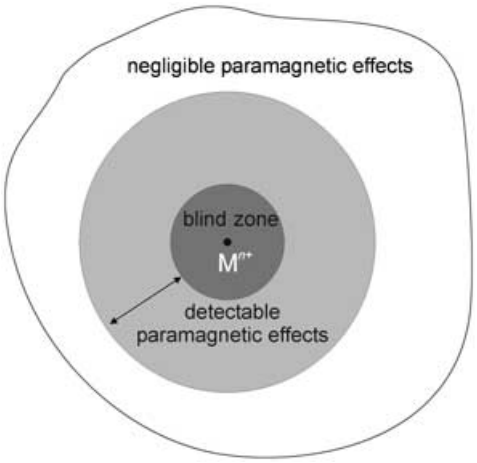

Figure 2. The inner sphere centered on the paramagnetic metal ion is a blind-zone, as proton NMR signals are too broad to be detected. Outside this sphere, there is another sphere indicating the region where NMR signals are visible and still affected by paramagnetism, so that information can be extracted on their position with respect to the metal ion.

Ivano Bertini was born in 1940, obtained the Italian degree of Doctor in Chemistry at the University of Florence in 1964 and then the Libera Docenza in 1969. He became a full Professor in General and Inorganic Chemistry in 1975 at the University of Florence where he is now. He received the Laurea Honoris Causa from the University of Stockholm in 1998, the University of Ioannina in 2002, and the University of Siena in 2003. He is a physical inorganic chemist who has cultivated NMR spectroscopy since 1965. He is a founder and director of the Center of Magnetic Resonance (CERM), an NMR-spectroscopy-based infrastructure operating in the field of life sciences.

Giacomo Parigi is researcher at the University of Florence. He graduated in physics cum laude at the University of Florence in 1992 and obtained a PhD in Chemistry at the University of Florence in 2000. He is the author of 36 publications in international scientific journals and of a book, together with I. Bertini and C. Luchinat, on Solution NMR of Paramagnetic Molecules. *His research activity is mainly oriented to the study of the effects due to paramagnetic metal ions on nuclear relaxation and on the NMR signals of metal-containing proteins.*

Claudio Luchinat is Professor of Chemistry at the University of Florence. He graduated in chemistry cum laude at the University of Florence in 1976 and has been a full Professor in General and Inorganic Chemistry since 1986. He is the author of more than 400 publications in scientific journals of international reknown and of five books on NMR spectroscopy of metalloproteins and nuclear and electron relaxation. His research interests are mainly in structural biology, metalloproteins and metalloenzymes, the theory of electron and nuclear relaxation, relaxometry, and contrast agents for magnetic resonance imaging.

Roberta Pierattelli is Associate Professor of Chemistry at the University of Florence. She graduated in chemistry in 1990 and she got a PhD in Chemistry at the same University in 1995. Her research interests are mainly devoted to the study of the structure and function of metalloproteins and metalloenzymes by NMR spectroscopy.

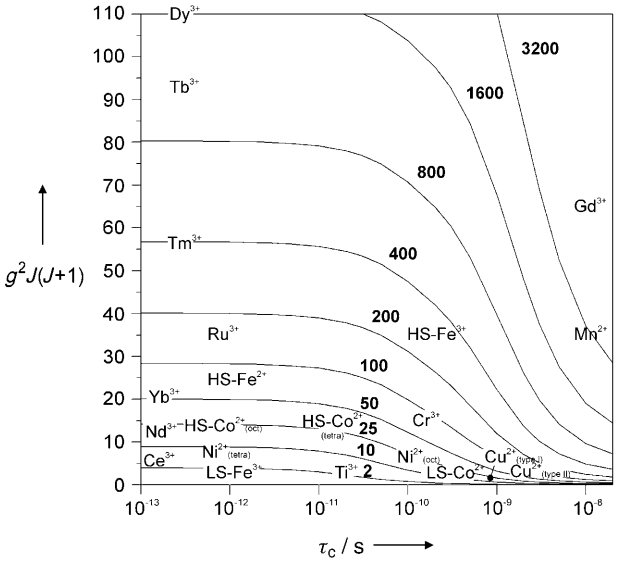

Figure 3. The extent of line broadening at 900 MHz experienced by a proton 10 Å away from the metal in a protein of $M_W = 25\,000$ Da (rotational correlation time, $\tau_r = 10^{-8}$ s) at 298 K depends on the nature of the metal ion, that is, on the number of unpaired electrons and on its electron relaxation time. Solid lines indicate the values of $g^2J(J+1)$ and correlation time τ_c with constant R_2 values ($R_2 = \pi\Delta\nu$), where g is the free electron g_e factor or the g_J factor for lanthanides and actinides (Ce: $^6/_7$, Nd: $^9/_2$, Dy: $^4/_3$, Tb: $^3/_2$, Yb: $^8/_7$, Tm: $^7/_6$), J is the S quantum number or the $L+S$ quantum number for lanthanides and actinides, and τ_c is calculated as $1/(\tau_r^{-1}+\tau_s^{-1})$, with τ_s being the electron relaxation time. HS stands for high spin and LS for low spin.

This article deals with 1) the best exploitation of the information contained in the broadening of the lines and 2) the improvement of the observability of broad signals. The paramagnetic broadening of lines contains much information on the electron–nucleus hyperfine coupling and ultimately includes the metal ion in a network of restraints involving part of the protein. Therefore, in favorable cases, the solution structure can be obtained based only on NMR data and, more often, the protein part may be better defined than in the case of diamagnetic proteins. In fact, studies that exploit a paramagnetic metal ion intentionally bound to a protein are many in the literature and are quite fashionable.[22–35]

2. Paramagnetism-Based Structural Restraints in Solution

2.1. Hyperfine shift

Contact shift: The NMR lines affected by the presence of unpaired electrons may easily experience an extra contribution to the chemical shift, which is called hyperfine shift. If the unpaired electron can delocalize onto the resonating nuclei, then these experience the so-called *contact* or *Fermi contact shift* (δ^c). This shift contains structural information; however, it is hidden inside the particular mechanisms of unpaired-electron delocalization. No general protocols are available for solution structure determination, but several attempts can be found in the literature[36–53] for the use of such effects in specific cases. Examples are the use of contact shifts on the β-CH_2 protons of cysteine residues coordinated to iron(II)/iron(III) ions in iron–sulfur proteins to provide dihedral-angle information through Karplus type relationships (Figure 4 A)[37] or the use of contact

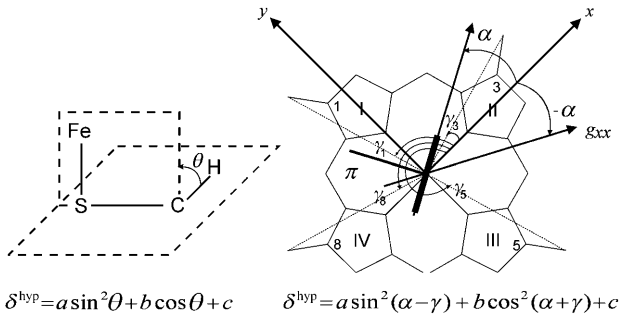

Figure 4. A) Karplus relationship for Hβ nuclei of iron-coordinated cysteines in proteins containing Fe–S clusters. B) Karplus relationship for low-spin iron(III) heme methyl groups in histidine–cyanide cytochromes.

shifts (or combinations of contact and pseudocontact shifts, see below) of methyl protons in heme proteins containing low-spin iron(III) ions to determine the orientation of the axial ligand(s) (Figure 4 B).[36,38,39,42,43,47,48,54] In all cases, the use of contact shifts is parametric, as their quantomechanical calculation from first principles is not trivial. Calculations by means of a high-level hybrid density-functional treatment were performed on the protein rubredoxin, a small protein containing a single iron center coordinated to four cysteinate sulfur atoms. A remarkably good agreement with the experiments was obtained.[46,53] The paramagnetism has a strong effect on the nuclei close to the iron center, thereby leading to extreme line broadening and very large hyperfine shifts.[55]

Often, the electron magnetic moment is anisotropic, that is, it takes up different values for different orientations of the protein in the external magnetic field. Under these conditions, the dipolar coupling with the nuclear spin magnetic moment does not average zero upon rotation, because the electron magnetic moment vector is not constant. This nonzero average of the dipolar coupling energy produces a contribution to the hyperfine shift, which is called the *pseudocontact shift* (δ^{pcs}). In principle, each nucleus in a paramagnetic protein may experience a sum of contact and pseudocontact shifts. However, with a bit of chemical intuition, it is possible to decide at first glance which nuclei experience only pseudocontact shift and not contact shift: for example, if the number of chemical bonds separating the resonating nucleus from the metal ion is larger than four and there are no π bonds, the contact shift can be considered negligible and any observed hyperfine shift can be considered to be pseudocontact in nature. This is a great advantage, as the δ^{pcs} measurement directly contains valuable structural information (see below). In some cases, strong deviations from the predicted δ^{pcs} values for nuclei in the vicinity of the metal ion can be taken as evidence of contact shifts, that is, of the presence of through-bond connectivities. For example, in the case of the protein calbindin D_{9k}, a calcium-binding protein where the calcium(II) ion in the C-terminal site can be selec-

tively substituted with lanthanides, the analysis of the hyperfine chemical shifts induced by Ca^{2+} substitution with Ce^{3+} on several CO groups revealed contact contributions due to direct binding to the metal ion. This allowed the unambiguous identification of the metal ligands.[56]

Pseudocontact shift: Pseudocontact shifts were described as early as 1958,[57] but the first attempts to use them to refine a protein structure in solution by starting from X-ray data appeared in 1995.[58] Eventually a protocol for solution structure determination appeared the following year. The δ^{pcs} values are given by Equation (1)[59], where r is the distance between observed nuclei and metal ion, and $\Delta\chi_{ax}$ and $\Delta\chi_{rh}$ are the axial and rhombic anisotropy parameters of the magnetic susceptibility tensor of the metal, as defined by Equation (2), and θ and φ identify the polar coordinates of the nucleus in the frame of the electronic magnetic susceptibility tensor.

$$\delta^{pcs} = \frac{1}{12\pi r^3}\left[\Delta\chi_{ax}(3\cos^2\theta - 1) + \frac{3}{2}\Delta\chi_{rh}\sin^2\theta\cos 2\varphi\right] \quad (1)$$

$$\Delta\chi_{ax} = \chi_{zz} - \frac{\chi_{xx}+\chi_{yy}}{2} \text{ and } \Delta\chi_{rh} = \chi_{xx} - \chi_{yy} \quad (2)$$

Pseudocontact shifts thus depend on the 3rd power of the metal-to-nucleus distance, and the extent of the magnetic susceptibility anisotropy sets the radius of the sphere where the hyperfine shifts are measurable. Equation (1) resembles a d orbital function as it is taught in freshman chemistry courses (more precisely, a d_{z^2} function if $\Delta\chi_{rh} = 0$ or a $d_{x^2-y^2}$ function if $\Delta\chi_{rh} = {}^2/_3\Delta\chi_{ax}$; Figure 5). Therefore, a value of pseudocontact

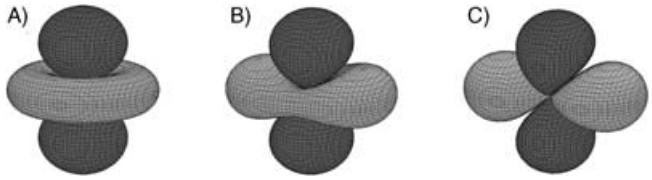

Figure 5. Isopseudocontact shift surfaces calculated from Equation (1) with A) $\Delta\chi_{rh} = 0$, B) $\Delta\chi_{rh} = {}^1/_3\Delta\chi_{ax}$, and C) $\Delta\chi_{rh} = {}^2/_3\Delta\chi_{ax}$. Positive shifts are in dark gray, negative shifts in light gray. Note the resemblance of the surfaces in A and C to the d_{z^2} and $d_{x^2-y^2}$ orbitals, respectively.

shift corresponds to an infinite number of nuclear coordinates in the metal magnetic susceptibility anisotropy coordinate system, that is, all the positive or negative points of the surface of a d orbital (Figure 5). Therefore, the δ^{pcs} information alone cannot solve a structure. However, it was shown that the δ^{pcs} values are absolutely consistent with NOEs and dihedral-angle structural restraints.[60–62] A protocol has been thus implemented to include these restraints in the most popular software packages for solution structure determination, such as DYANA/CYANA[63,64] and Xplor-NIH.[65] Although such programs are not optimized for handling these restraints, due to the complicated form of the energy surface, they have been shown to be precious not only for protein refinement but also for ab initio structural calculations.[64]

In general, the δ^{pcs} values can be measured after the complete assignment of the ^1H,^{15}N-HSQC spectra of both the diamagnetic and the paramagnetic samples is obtained. However, when the assignment of the diamagnetic spectrum is available, a shortcut is possible.[28] In fact, the signals of nuclei far from the metal ion have small δ^{pcs} values and the corresponding signals resonate close to the diamagnetic ones. For some isolated resonances, the assignment can be easily transferred from one spectrum to another, and a first estimate of the tensor is possible from this subset of δ^{pcs} values. A much larger number of δ^{pcs} values can then be found from the comparison of observed and calculated values for additional resonances, and the process can be repeated.

The first application of this technique was on a low-spin iron(III) heme protein.[61] Low-spin iron(III) has one unpaired electron and significant magnetic anisotropy.[48,66] If we know the hyperfine shifts, that is, the differences in shift between the actual paramagnetic system and the analogous diamagnetic system for nuclei of residues not experiencing any contact shift, then we know the δ^{pcs} values. At this point, we may rely on a preliminary structure to extract the polar coordinates for each proton with respect to an arbitrary internal-axes frame, and we then find, through Equation (1), the $\Delta\chi_{ax}$ and $\Delta\chi_{rh}$ values and the three independent direction cosines that define the principal directions of the magnetic anisotropy tensor with respect to the internal axes.[67–69] The inclusion of this piece of information in the calculation protocol, together with all the other restraints available, such as upper distance limits derived from NOE data, permits a better definition of the structure itself.[25,60,62,70–75] In the case of Ala80Met Cyt *c*,[61] for example, the refinement of the structure calculated with the standard approach, reported in Figure 6A, shows some not very well-defined regions, in particular in the heme cleft. With the inclusion of the restraints obtained from the analysis of the δ^{pcs} values, the quality of the structure improved, as shown in Figure 6B.

Pseudocontact shifts can be used also as restraints in molecular dynamics. A module[76] is available for the popular program Amber.[77] A novel strategy for fast resonance assignment of ^1H,^{15}N HSQC spectra based on pseudocontact shifts was also proposed.[78]

Most of the data used in structural refinements involve ^1H δ^{pcs} values, although ^{15}N and ^{13}C δ^{pcs} values are also used.[23,62,79] Since δ^{pcs} values are calculated as the difference between the chemical-shift values observed for the nuclei in a paramagnetic system and in a diamagnetic analogue, the latter is obtained by removing the paramagnetic ion, by substituting the paramagnetic metal ion with a diamagnetic metal, or by reducing the paramagnetic metal to a diamagnetic state.

It is worth mentioning that ^1H δ^{pcs} values are always in excellent agreement with other constraints, that is, the values back-calculated from the resulting structure match very well with the measured ones. On the contrary, when the diamagnetic analogue used to calculate the pseudocontact shifts is the same metal in a different oxidation state, for instance, low-spin iron(II) as a diamagnetic analogue for low-spin iron(III) in a heme protein, heteronuclear (^{13}C[80–82] and ^{15}N[81,83,84]) δ^{pcs} values may show small but significant deviations. The origin of these

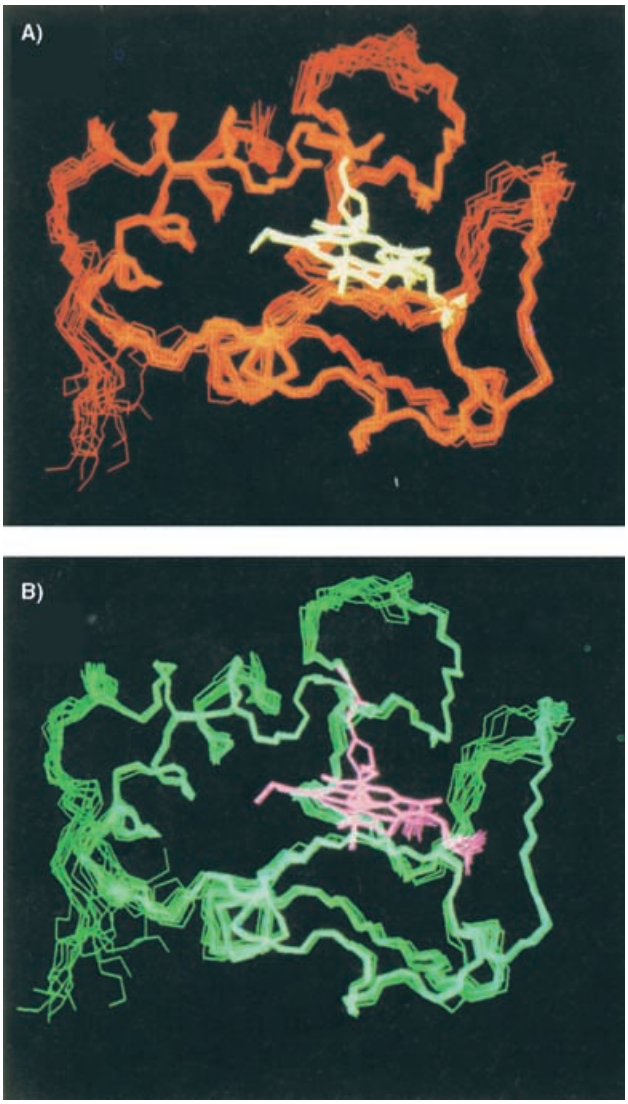

Figure 6. Solution structure of the *Saccharomyces cerevisiae* Met80Ala iso-1-cytochrome *c*. The 17 best structures of A) the original DIANA family and B) the final PSEUDIANA family are compared.

deviations, dubbed *redox shifts*, is not understood yet. Contact contributions can be ruled out for nuclei of residues not bound to the metal ion. Among the possible causes that have been considered are slight differences in the structure of the protein in the two oxidation states, long-range electrostatic effects due to the different overall charge of the molecule, and even long-range electron delocalization effects that may render partially invalid the point-dipole approximation used to treat all electron–nucleus coupling phenomena. When this happens, either the allowed tolerance in the calculation is increased or the restraints are dropped.

2.2 Relaxation rates

Longitudinal and transverse nuclear relaxation rate enhancements (R_1 and R_2, respectively) in paramagnetic proteins generally depend on the dipolar coupling between the unpaired electron and the resonating nuclei. The relevant equation for the *longitudinal dipolar relaxation rate enhancement*, R_{1para}, is in the form of Equation (3):[85], where rates k_1 and k_2 depend on the observed nuclear species, on the electron spin quantum number, on the proton Larmor frequency ($\omega_I = \gamma_I B_0$) and on the correlation times related to the mechanisms responsible for relaxation.

$$R_{1para} = \frac{k_1 + k_2}{r^6} \quad (3)$$

The k_1/r^6 value is proportional to the square of the dipole–dipole interaction between the nuclear spin and the electron spin, and it contains the correlation time, τ_c, which is defined by Equation (4). From this equation it appears that τ_c is dominated by the shortest among the electron relaxation times, τ_s, the protein rotational correlation time, τ_r, and the exchange time, τ_M, which may enter the picture if either the nucleus or the metal belong to chemical moieties that are in chemical exchange with the protein. In metalloproteins, τ_c is usually equal to τ_s.

$$\tau_c^{-1} = \tau_s^{-1} + \tau_r^{-1} + \tau_M^{-1} \quad (4)$$

The quantity k_2/r^6 is proportional to the square of the dipole–dipole interaction between the nuclear spin and the time-average of the electron magnetic moment, called the *magnetic susceptibility relaxation*[21] or *Curie spin relaxation*.[20] It contains a correlation time which is given by the shortest value between τ_r and τ_M. In metalloproteins, it is usually equal to τ_r. The k_2 value is usually negligible with respect to the k_1 value in the case of R_1 data but not in the case of R_2 data (see below).

Equation (3) shows that the relaxation rate enhancement effects depend on the inverse of the 6th power of the metal-to-nucleus distance, thus they tend to vanish rapidly. As anticipated in Section 1, they are measurable in a spherical shell from the metal (Figure 2) where the effect is not too weak to be negligible and not too strong to make the signals unobservable. To be used as structural constraints, the relaxation rate enhancements need to be extracted from the relaxation rates in the paramagnetic protein and the relaxation rates of a diamagnetic analogue. Sometimes, instead of measuring the individual diamagnetic relaxation rates, an average diamagnetic value can be calculated, and an upper value can be taken to be subtracted from the experimental R_1 value in order to obtain a lower limit for the R_{1para} value, which is a good upper distance limit restraint. We use such upper distance limits as restraints in our protocols (www.postgenomicnmr.net) for solution structure determination. The rationale for doing this instead of direct refinement against rate enhancements, is that the experimental uncertainty on relaxation rates is roughly proportional to the rates themselves. Therefore, direct refinement tends to overestimate the contribution of large rates to the target function, which is minimized by the program for structure determination. As distances depend on the inverse sixth root of the rates, the use of distances is less biased.

In Figure 7, the improvement around the iron–sulfur cluster II in the solution structure of oxidized ferredoxin, a protein

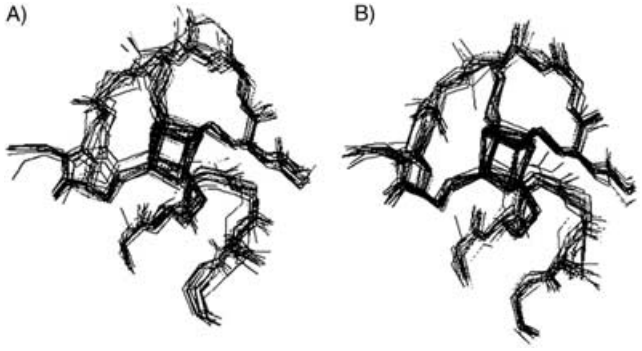

Figure 7. Solution structure of *Clostridium pasteurianum* ferredoxin in the proximity of iron–sulfur cluster II.[86] A) Family obtained by using NOE data only and B) family obtained after addition of relaxation rate restraints.

containing 55 amino acids and 2 [4Fe–4S] clusters, upon inclusion of 69 new restraints based on R_1 measurements is shown.[86]

Similarly to the R_1 value, the transverse nuclear relaxation rate enhancement, R_{2para}, is defined by Equation (5).

$$R_{2para} = \frac{k_1\prime + k_2\prime}{r^6} \tag{5}$$

The contribution to R_2, and thus to line widths, of the term due to Curie relaxation is often very important in paramagnetic metalloproteins, especially at high magnetic fields, due to its dependence on the large value of the rotational correlation time, τ_r.[85] R_2 restraints have been used for structural calculations, for example, in spin-labeled platinum complexes, to better define the bending of the DNA duplex as an adduct with a platinum complex,[87] in spin-labeled RNA, for the determination of the structure of protein–RNA complexes,[88] in ubiquitin tagged with a three-residue copper(II)-binding sequence, and to extract distance restraints.[24]

2.3. Cross-correlation between Curie and dipolar relaxations

Modulation of nuclear dipole interaction with both another nuclear dipole and the average induced electron dipole, present in paramagnetic systems, causes relaxation. When both modulations are operative, cross-correlation between the two relaxation mechanisms occurs because the two relaxation mechanisms have the same correlation time, that is, the rotational correlation time, τ_r. Such cross-correlation causes differential line broadening in coupled signals, since in a two-spin system it increases the line width of one component and decreases by the same extent the line width of the other component. As an example, the total difference in line width between the two signal components (in Hz) in the proton dimension of the HN doublet is defined by Equation (6).[89] The angle θ is that between the H–N axis and the proton–metal axis, r is the distance between the proton and the metal ion, and the other symbols have the standard meanings. For lanthanides and actinides, g_e is replaced by g_J and S by J.

$$\Delta(\Delta\nu_{1/2}) = \left(\frac{\mu_0}{4\pi}\right)^2 \frac{B_0\gamma_H^2\gamma_N\hbar\mu_B^2 g_e^2 S(S+1)}{15\pi kTr^3 r_{HN}^3}(3\cos^2\theta - 1)\left(4\tau_r + \frac{3\tau_r}{1+\omega_I^2\tau_r^2}\right) \tag{6}$$

Protocols for the use of Curie dipolar relaxation *cross-correFlation rate restraints* (ccrs) are available at the web site www.postgenomicnnmr.net for the programs PARAMAGNETIC DYANA/CYANA[64,90] and Xplor-NIH.[65]

Paramagnetic cross-correlation effects were first discussed in 1993,[91,92] measured for HN metalloproteins in 1999,[93] and have been used as restraints since 2000.[94–96] We show here the example of Met-aquomyoglobin. This is a protein containing a high-spin iron(III) ion ($S = {}^5/_2$), which determines large Curie relaxation rates, thus causing large signal line widths. These conditions make a meaningful use of δ^{pcs} and residual dipolar coupling (see Section 2.4) restraints particularly difficult. Paramagnetic cross-correlation restraints could thus be profitably used for protein solution structure determination. Paramagnetic ccr values were measured for 61 amide protons, ranging from −6.8 to 9.1 Hz, at distances between 9.7–28.5 Å from the metal.[97] The effect of cross-correlation between Curie relaxation and chemical shielding anisotropy (CSA) was recently investigated.[98]

The imaginary part of the spectral density related to the same cross-correlation effect causes the so-called dynamic frequency shift. It can contribute to the difference between the ^1J values of the paramagnetic and diamagnetic species, for instance, of the HN doublet, according to Equation (7), first published in a complete form in ref. [65]. In this equation, the angle θ_{Sij} (i,j = H,N) is that between the ij axis and the i–metal-ion axis, r_{iS} is the i–metal-ion distance, and ω_N is the nitrogen Larmor frequency multiplied by 2π.

$$\Delta\nu_{DFS} = \left(\frac{\mu_0}{4\pi}\right)^2 \frac{B_0\gamma_H\gamma_N\hbar\mu_B^2 g_e^2 S(S+1)}{5\pi kT} \times \left(\frac{\gamma_H}{r_{HN}^3 r_{HS}^3}\frac{3\cos^2\theta_{SHN}-1}{2}\frac{\omega_I\tau_r^2}{1+\omega_I^2\tau_r^2} + \frac{\gamma_N}{r_{HN}^3 r_{NS}^3}\frac{3\cos^2\theta_{SNH}-1}{2}\frac{\omega_N\tau_r^2}{1+\omega_N^2\tau_r^2}\right) \tag{7}$$

Such a contribution to the ^1J value is small (with respect to residual dipolar coupling values; see Section 2.4) and decreases with the third power of the distance between the observed nuclei and the metal ion. In any case, the overall paramagnetic dynamic frequency shift contribution to the ^1J value is expected to be negligible and can be safely not taken into account in the structural calculations.

2.4. Residual dipolar couplings

The ^1J splitting of coupled nuclei can experience a dipolar contribution, due to partial orientation of the investigated system in the magnetic field. Such a contribution is called *residual dipolar coupling* (rdc). Partial orientation can be achieved by dissolving the investigated molecules in solutions containing orienting devices[99] or can be due to intrinsic anisotropy of the

magnetic susceptibility tensor (self-orientation).[100] In the latter case, the different energies related to each orientation of the magnetic field with respect to the magnetic susceptibility tensor (Figure 8) in fact cause different probabilities for the orientations to occur in the presence of sizable anisotropy of the latter; thus, nucleus–nucleus dipolar couplings do not average zero. A small anisotropy of the magnetic susceptibility tensor is also present in diamagnetic proteins but is usually too small to be usable, while it can be very large in paramagnetic systems. For a given magnetic susceptibility anisotropy, self-orientation increases with the square of the external magnetic field. Paramagnetic rdc values were first used for solution structure determination in 1998 for the protein cytochrome b_5 in both the oxidized and reduced forms.[101] These new restraints were calculated according to Equation (8), which took into account both the contributions of the axial and rhombic anisotropies for the first time.[59,101]

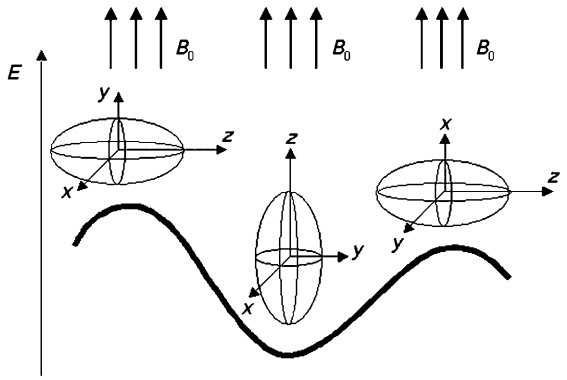

Figure 8. The energy of a magnetically anisotropic molecule depends on the orientation of the protein with respect to the magnetic field, B_0.

$$\Delta\nu_{RDC}(\mathrm{Hz}) = -\frac{1}{4\pi}\frac{B_0^2}{15kT}\frac{\gamma_N\gamma_H\hbar}{2\pi r_{HN}^3}\left[\Delta\chi_{ax}(3\cos^2\theta-1)+\frac{3}{2}\Delta\chi_{rh}\sin^2\theta\cos 2\phi\right] \quad (8)$$

The equation resembles that for pseudocontact shifts, but it is actually very different: in this case, the distance r_{HN} is that between the two coupled nuclei and is usually fixed, and the polar angles θ and ϕ are those defining the orientation of the vector connecting the coupled nuclei in the frame of the magnetic susceptibility tensor. Therefore, rdc values are not related at all to the position of the coupled nuclei with respect to either the metal ion or the magnetic susceptibility tensor; instead, they depend only on the orientation of the vector connecting the coupled nuclei.[100,102–104] By contrast, δ^{pcs} values depend on the position of the nuclei with respect to both the metal ion and the paramagnetic susceptibility tensor, besides the value of the anisotropies of the latter.

For paramagnetic molecules, ^1J splittings are often measured for both the paramagnetic system and a diamagnetic analogue. Such an approach provides the precious advantage that the difference in the splitting between the paramagnetic and the diamagnetic signals is only related to paramagnetism, and the anisotropies in Equation (8) are those related to the paramagnetic susceptibility tensor, that is, they are the same as those of Equation (1) describing the pseudocontact shifts. Therefore, Equation (8) is usually employed with the $\Delta\chi_{ax}$ and $\Delta\chi_{rh}$ parameters fixed according to the values obtained from the analysis of the pseudocontact shifts, which are more suitable for the correct determination of such parameters as they depend much less than residual dipolar couplings on possible local motions in the protein. This approach is correct as long as dynamic frequency shift can be neglected (see Section 2.3).

In summary, the greatest advantage in the use of the paramagnetic rather than diamagnetic rdcs is the fact that an independent and accurate estimate of the magnetic anisotropy tensor parameters is available from δ^{pcs} values. As already described in Section 2.1, a robust estimate of the tensor parameters can usually be obtained quickly. It is not always fully appreciated that, relying on best-fit estimates of the magnetic anisotropy tensor parameters from the rdcs themselves, as is done when external orienting systems are used, may lead to the underevaluation of the possible presence of extensive local motions. The analysis of motions in such cases has been shown to be possible only when the rdcs are measured for least five different alignments.[105,106]

If a diamagnetic reference cannot be conveniently used, the rdc values can also be obtained by performing measurements on the same paramagnetic sample at two different magnetic field strengths. In this way, it is possible to get the differences in ^1J splitting of coupled nuclei, which can be calculated according to Equation (8) with B_0^2 replaced by the difference between the two squared magnetic fields. The magnetic susceptibility anisotropies in Equation (8) are, in this case, related to the overall molecular magnetic susceptibility tensor, which comprises both a diamagnetic and a paramagnetic term and are thus different from those relevant for δ^{pcs} calculations. Actually, the first use of rdcs as structural restraints was implemented according to this procedure,[101] with the resulting susceptibility tensor of the oxidized cytochrome b_5 in good agreement with that expected from the diamagnetic susceptibility tensor of the reduced protein and the paramagnetic susceptibility tensor obtained from pseudocontact shifts.

For both diamagnetic and paramagnetic rdcs, a large number of sharp local minima can cause difficulty in handling single sets of rdc restraints for solution structure determination in simulated annealing minimization programs.[94,107,108] In the case of metalloproteins, substitution of different paramagnetic ions can be performed to vary the paramagnetic susceptibility tensor and, thus, to obtain different sets of rdcs. If more than one rdc value is available for a given internuclear vector, the degeneracy is strongly decreased; if three or more rdc values are available, the number of orientations that simultaneously solve Equation (8) is reduced to only two (opposite to one another). When several sets of self-orientation residual dipolar couplings are available, rdc restraints can be much more efficiently used by directly providing as restraints in the structure calculations the polar θ and ϕ angles describing the orienta-

tion of the vector connecting the pairs of coupled nuclear spins with respect to an arbitrary reference frame. This approach was shown to work in the case of the protein calbindin D_{9k} where the calcium(II) ion in the C-terminal site was selectively substituted with Ce^{3+}, Tb^{3+}, Dy^{3+}, Ho^{3+}, Er^{3+}, Tm^{3+}, or Yb^{3+}.[109]

Protocols are available at the web site www.postgenomic nmr.net for the profitable use of rdc values in conjunction with δ^{pcs} values and the other paramagnetism-based restraints by employing the programs PARAMAGNETIC DYANA/CYANA[63] or Xplor-NIH.[65]

2.5. Simultaneous use of paramagnetism-based restraints

As already pointed out, all the paramagnetism-based restraints (δ^{pcs}, R_{1para}, paramagnetic ccrs, self-orientation rdcs) have been experimentally demonstrated to be consistent with one another and with the NOEs, the dihedral angles based on ^3J values, and the other diamagnetic restraints. The protein calbindin D_{9k} has been used to demonstrate the simultaneous use of all of them. From 1823 NOEs, 191 dihedral angles, 15 hydrogen bonds, 1738 δ^{pcs} values related to 11 lanthanides, 64 self-orientation rdc values, 26 R_1 values, and 47 paramagnetic ccr values, a family with a backbone root mean square deviation (RMSD) from the mean of less than 0.3 Å was obtained.[23,90,110,111] The backbone RMSD from the mean of the family obtained with the diamagnetic restraints was 0.7 Å. Figure 9 shows the two

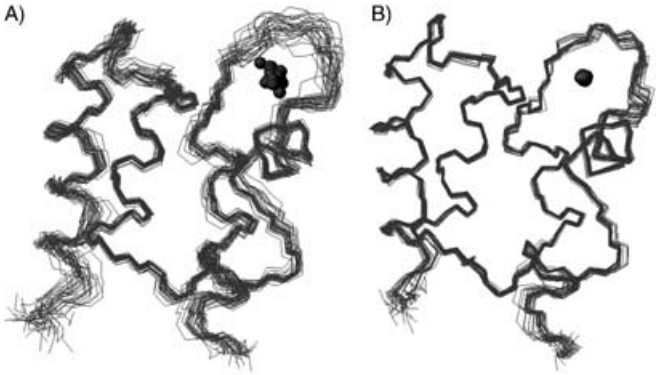

Figure 9. A family of 30 conformers of calbindin D_{9k} obtained A) with diamagnetic restraints only and B) with the addition of paramagnetism-based restraints.[23]

families (30 structures) calculated without and with the inclusion of the paramagnetism-based restraints. It was also shown that paramagnetism-based restraints, together with identification of the secondary structure elements, may provide the backbone solution structure of a metalloprotein even in the absence of any NOEs.[64,94,108]

In conclusion, paramagnetism-based restraints have been proven to be precious for the solution structure determination of paramagnetic proteins. This is particularly true if, for any reason, the number of NOEs is limited. Each class of restraints provides a different type of structural information. Paramagnetic relaxation enhancements provide information on the distance between the observed protein nuclei and metal ion and are thus quite similar to the NOE restraints, although all distances are referring to the same atom. Cross-correlations between Curie and dipolar relaxations provide information on the distance of each observed nucleus from the metal ion and on the angle between its coupled-nuclei direction and the metal-ion direction. Pseudocontact shifts provide information on the distance of the observed nuclei from the metal ion and on their orientation with respect to the paramagnetic susceptibility tensor. Self-orientation residual dipolar couplings provide information on the orientation of coupled nuclei with respect to the paramagnetic susceptibility tensor and are independent on their position with respect to the metal ion. δ^{pcs} values and paramagnetic relaxation enhancements can be used profitably in ab initio structural calculation; cross-correlations can also be used from the early steps, being weighted with force constants proportional to r^3, where r is the distance between the observed nuclei and the metal ion. Residual dipolar couplings are more useful when several sets (>2) of self-orientation residual dipolar couplings are available, as obtained from measurements on the same molecule when different paramagnetic metal ions are alternatively bound to the same binding site. In such a case, in fact, they can be used to calculate the polar angles describing the orientation of the vector connecting a pair of coupled nuclear spins with respect to an arbitrary reference frame.[109] Such information can be straightforwardly introduced in structure calculation algorithms, thus making the use of the residual dipolar couplings restraints more efficient.

In Table 1 some typical values of the paramagnetism-based restraints at 900 MHz have been reported for different metal ions. All data are calculated for a proton located 10 Å from the paramagnetic ion and assumed to be in a protein scaffold with a reorientational time of 10^{-8} s (about 25 000 Da) at 298 K. Pseudocontact shifts, NH residual dipolar couplings, and NH cross-correlations are reported as the extreme (absolute) values, calculated in the axial assumption, that is, for a proton along the z axis of the metal susceptibility tensor and a coupled nitrogen atom along the metal–proton direction. Typical values for the electron relaxation time (also shown in Figure 3), as well as of the axial anisotropy of the magnetic susceptibility tensor, used for estimating the values of the restraints, are also reported, together with the values of the electron spin quantum number S (or of $J=L+S$ for lanthanides).

It is expected that paramagnetism-based restraints are usable in large molecules and possibly in solid-state NMR spectroscopy. An important feature when dealing with large molecules is that, in Equation (5), an increase in τ_r[85] and the paramagnetic effect leads to an increase in the region in which proton NMR lines are too broad to be detected. Efforts were thus made in order to increase the shell in which signals are observable, particularly in the region close to the metal ion. This was performed by detecting signals of nuclei other than protons. Finally, paramagnetism-based restraints can provide structural information not otherwise available. This has been shown clearly in the case of calmodulin, a two-domain protein experiencing large conformational freedom.[112] The combined use of δ^{pcs} and rdc values in one domain that originated from

Table 1. S (or J) values for selected metal ions, typical values for the electron relaxation time, τ_s, and for the axial magnetic susceptibility anisotropy, $\Delta\chi_{ax}$, at 900 MHz and 298 K.[85,146] The extreme (absolute) values of the paramagnetism-based restraints calculated with Equations (1), (3)–(6), and (8) for a proton at 10 Å, with $\tau_r = 10^{-8}$ s, are also given.

Metal ion	S or J	τ_s [10^{-12} s]	$\Delta\chi_{ax}$ [10^{-32} m^3]	R_{1para} [s^{-1}]	R_{2para} [s^{-1}]	R_2^{Curie} [s^{-1}]	$\delta^{pcs[a]}$ [ppm]	rdc[b] [Hz]	ccr[c] [Hz]
Fe^{III} HS[d]	5/2	100	3.0	65	241	152	1.6	4.2	54
Fe^{III} LS[d]	1/2	1	2.4	0.09	1.22	1.12	1.3	3.4	4.6
Fe^{II}	2	1	2.1	0.72	72.3	71.6	1.1	2.9	37
Co^{II} HS[d] tetracoord.	3/2	10	3	3.7	32.3	28.0	1.6	4.2	23
Co^{II} HS[d] esacoord.	3/2	1	7	0.44	28.4	28.0	3.7	9.8	23
Cu^{II}	1/2	3000	0.6	1.0	115	1.1	0.3	0.8	4.6
Gd^{III}	7/2	10000	0.2	9.9	5668	493	0.1	0.3	97
Ce^{III}	5/2	0.1	2	0.05	5.2	5.1	1.0	2.8	10
Dy^{III}	15/2	0.5	35	2.9	1600	1596	19	49	175
Tb^{III}	6	0.3	35	1.94	1111	1109	19	49	146
Yb^{III}	7/2	0.3	7	0.33	52.9	52.6	3.7	9.8	32
Tm^{III}	6	0.5	20	1.26	407	406	11	28	88

[a] Calculated for a proton in an axial position with respect to the χ tensor ($\theta = 0$), see Equation (1). [b] Calculated for the N–H pair, oriented along the z axis of the χ tensor ($\theta = 0$), see Equation (8). [c] Differential line width calculated for a N–H pair oriented along the direction comprising the metal ion ($\theta = 0$), see Equation (6). [d] HS = high spin, LS = low spin.

paramagnetic metals in the other domain allowed us for the first time to sample and quantify the conformational space experienced by the protein, that is, to obtain structural information in the absence of a defined structure. The method can, in principle, be generalized to other multidomain proteins.

3. The Use of Heteronuclear NMR Spectroscopy

To increase the shell of observable signals, ^{13}C direct-detection NMR spectroscopy is advantageous, as the dipolar contributions to nuclear relaxation depend on the square of the magnetogyric ratio of the observed nucleus, and a decrease in relaxation rates by a factor of approximately 16 occurs on changing from ^{1}H to ^{13}C detection. Of course, there is a concomitant reduction of sensitivity, as the signal-to-noise ratio of a spectrum depends on the $^{5}/_{2}$ power of the magnetogyric ratio. However, the gain in resolution due to the reduced broadening of the NMR lines is such as to compensate, at least partially, for the loss in sensitivity.[113] Furthermore, improvements in hardware aim at increasing sensitivity in ^{13}C detection. Indeed, several applications of ^{13}C direct detection to paramagnetic macromolecules have recently appeared in the literature.[52,56,114–120]

In order to avoid proton detection, a novel approach for spin-system assignment has been developed. As illustrated in Figure 10, the starting point of the assignment procedure is to correlate the backbone carbon nuclei through a CACO experiment. The CO is then connected to the C^{β} through a CBCACO experiment, while the C^{α} is connected to the remaining atoms of the side chain though a ^{13}C-TOCSY experiment. Once all the spin systems have been identified, the sequence-specific assignment is accomplished with a CANCO experiment that correlates the CO shift of one residue with the ^{15}N shift of the following residue and the C^{α} shifts of the one residue and the following residue.[121,122] The redundant information obtainable with a CON[123] experiment, which correlates the backbone CO carbon atom with the peptidic nitrogen atom of the following residue, provides further confirmation of the assignment obtained by ^{13}C correlation. This strategy also provides the assignment of Asp, Asn, Glu, and Gln carbonyl and carboxylate carbon atoms, as well as quaternary carbon atoms of aliphatic side chains.

With this set of experiments, which can be recorded in 3D to reduce signal overlap, it is possible to assign signals of nuclei as close as 8 Å to the metal ion,

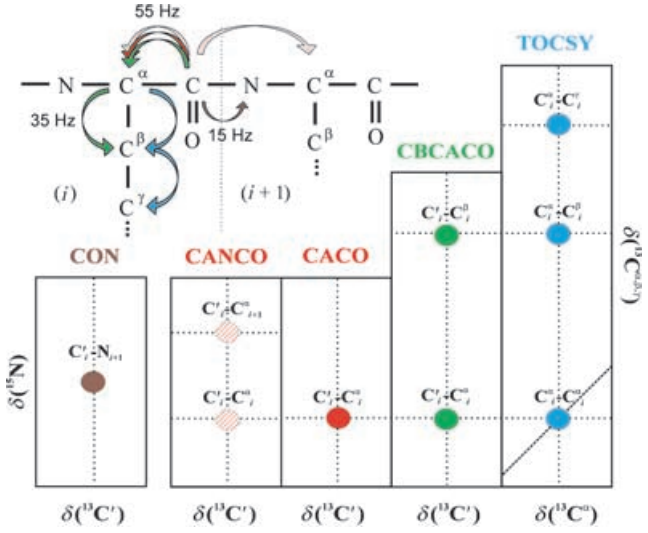

Figure 10. Illustration of the assignment procedure by ^{13}C NMR experiments only. The main J values for backbone nuclei are also reported.

even in the case of highly paramagnetic systems.[119] However, coherence transfer mechanisms become less effective as the line widths of the signals approach the value of the scalar coupling constant used for the transfer. In the case of one-bond carbon–carbon couplings, the $^{1}J_{CC}$ value is fairly large (35–55 Hz, see also Figure 10) but the paramagnetic R_2 contributions can overcome this range. This means that, to detect significantly broad signals, alternative experimental schemes should be used. As the paramagnetic contribution to relaxation is much less effective on longitudinal rates than on transverse rates, experiments in which magnetization is stored along the z axis are affected to a lesser extent by paramagnetic relaxation. This is the case for $^{13}C,^{13}C$ NOESY experiments, which promise to become the experiment of choice for the

assignment of the signals of nuclei in the coordination sphere of the metal ion.[118,119]

A characteristic feature of ^{13}C direct-detection NMR spectra is the presence of many homonuclear couplings that hamper the analysis of the spectra. For the CO signal the main coupling is with the C^{α}, which gives a relatively constant splitting of about 55 Hz. Several methods have been proposed to remove this splitting. Band-selective homodecoupling represents the most straightforward approach for *J*-splitting removal and it can be implemented in almost all of the pulse sequences.[118,124] However, when combined with ^{1}H and ^{15}N decoupling, it requires a four-channel spectrometer and the signal-to-noise ratio of the resulting spectra often suffers from some side effects implicit in the method. A more valuable approach is the inclusion in the experiments of in-phase/antiphase selection filters (IPAP).[125–127] The removal of the coupling is accomplished by recording two FIDs for each increment, one for the antiphase and one for the in-phase components; each pair of FIDs is then combined to separate the two multiplet components. These are then shifted to the center of the original multiplet (by $J_{COC}\alpha/2$ Hz) and summed to obtain a singlet.[128,129] In the case of spectra based on C^{α}-signal acquisition, from nuclei that generally present two large couplings (55 Hz with the CO moiety and 35 Hz with the C^{β} atom), a double in-phase/antiphase scheme can be implemented[128] to remove the double splitting. Other coupling patterns may be removed by selecting specific frequency ranges.

The potential of heteronuclear detection is nicely demonstrated in the case of Tb-substituted oncomodulin, a 109 amino acid protein containing 2 Ca^{2+} ions that can be selectively substituted with lanthanides.[119,130] When one of the two Ca^{2+} ions is substituted with Tb^{3+},[119] many backbone signals (more than 50%) are lost in the ^{1}H,^{15}N-HSQC spectrum[131] because of ^{1}H Curie relaxation (Figure 11), while only 37 out of 109 signals are lost in the CACO spectrum.[118] Tailored ^{13}C,^{13}C-NOESY spectra[119,128] with a relatively short mixing time and proper acquisition times allowed us to observe additional cross-peaks, thereby leaving a total of only 11 unobserved peaks out of 109. The 1D ^{13}C spectrum reveals very strongly shifted and very broad signals spread from $\delta = 270$ to -140 ppm. The assignment of these peaks is difficult in the absence of connectivities and also because their shifts are strongly dependent on small variations in geometry around the metal ion. However, some of them can be assigned from their predicted δ^{pcs} values, in a sort of iterative procedure, applicable in most cases. The assignment starts from some easily assigned ^{13}C signals experiencing a small contribution to the δ^{pcs} value, then the orientation of the magnetic anisotropy susceptibility tensor can be calculated to predict other observed shifts on the basis of the 3D structure, thereby allowing the assignment of other signals that are introduced in the new calculation and so on. Once the assignments are obtained, paramagnetism-based restraints may be conveniently used.

Aims in this field are those of making ^{13}C direct detection user-friendly and quick. Improvements in ^{13}C solid-state spectroscopy, where ^{13}C is the nucleus of choice, are beneficial to the development of direct detection of heteronuclei in solution. Optimization of the probes and the development of dedicated cryoprobes may definitely establish this technique as routine in NMR spectroscopy also for the diamagnetic proteins.

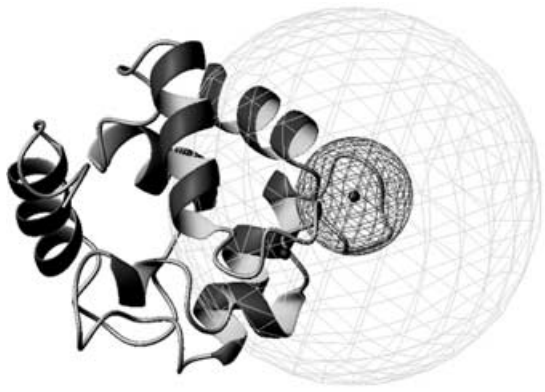

Figure 11. Display of the solution structure of rat oncomodulin (PDB file code: 1TTX). The light-gray sphere of radius 16 Å represents the region for which ^{1}H NMR signals are not detectable in the ^{1}H,^{15}N-HSQC spectrum due to the Tb-induced paramagnetic broadening. The dark-gray sphere of radius 5 Å identifies the limited region of space where some residues still remain unassigned with ^{13}C,^{13}C-NOESY experiments.

4. Conclusions and Perspectives

The first protein solution structure was published in 1985[132] and since then NMR spectroscopy has developed through diamagnetic-molecule applications. The broadening due to paramagnetism seemed an insurmountable obstacle for structure determination.[133] However, a few groups continued to deepen the understanding of the effects of hyperfine coupling in NMR spectroscopy and simultaneously to exploit technological advancements to increase the signal-to-noise ratio of paramagnetic-system spectra.[134–143] Eventually, a protocol for solving the structure of a paramagnetic metalloprotein was reported in 1994[144] and since then many examples have appeared in the literature.[63,145]

Of course, every metal ion has its own peculiarities and should be regarded as a case by itself. Low-spin iron(III) has already been mentioned: its sphere of nonobservability for proton NMR spectroscopy is quite narrow and its compounds represent the most popular class of paramagnetic compounds studied by NMR spectroscopy. Quite favorable is also cerium(III). Lanthanides are good and versatile paramagnetic probes that may substitute calcium. With the present technology, cerium(III) proteins can essentially be 100% assigned by ^{1}H NMR spectroscopy and the paramagnetism-based restraints are beneficial to the resolution of the structure. Other lanthanides (except gadolinium) have slightly larger regions where proton lines are broad, but with tailored experiments the assignment of large part of these resonances can be accomplished. These metal ions generally experience large magnetic anisotropy and therefore provide sizeable δ^{pcs} and rdc values that enable highly resolved solution structures to be obtained.

Gadolinium is known as a relaxing agent and consistently gives rise to a large blind-zone because both the k_1' and k_2' values in Equation (5) are large. ^{13}C direct detection alleviates the problem, but the blind-zone easily extends to 10–15 Å depending on the size of the molecules. In this case the pseudocontact shifts and the residual dipolar couplings are small because the magnetic anisotropy is small.

Similarly, high-spin iron(III) also has a large blind-zone which can be reduced by ^{13}C direct detection. The magnetic anisotropy is in this case of similar magnitude of that of low-spin iron(III), and paramagnetism-based restraints can be obtained in the visible region, which is however farther from the metal ion.

Copper(II) proteins represent a recent achievement in the field of solution structure determination. Copper(II) has only one unpaired electron but its k_1' value in Equation (5) is large and the region of the protein whose ^1H signals are broad is usually large. ^{13}C direct detection has reduced the blind-zone to the metal ligands, which are still undetectable because contact relaxation is prevalent there. The nonobservability of the ligands represents only a hint for their assignment as well.

In conclusion, much progress has been made in the case of paramagnetic molecules, both in the understanding of the subtle consequences of hyperfine coupling and in technological development in heteronuclear direct detection. More is expected to come.

Acknowledgements

This work was supported by the European Commission (contracts HPRI-CT-2001-50028 and QLG2-CT-2002-00988-SPINE), by MIUR-FIRB (contract RBAU013NSB) and by Ente Cassa di Risparmio of Florence.

Keywords: heteronuclear NMR experiments · metalloproteins · NMR spectroscopy · paramagnetism · protein structures

[1] C. Andreini, I. Bertini, A. Rosato, *Bioinformatics* **2004**, *20*, 1373 – 1380.
[2] H. M. Berman, J. Westbrook, Z. Feng, G. Gilliland, T. N. Bhat, H. Weissig, I. N. Shindyalov, P. E. Bourne, *Nucleic Acids Res.* **2000**, *28*, 235 – 242.
[3] E. Wörgötter, G. Wagner, M. Vasak, J. H. Kägi, K. Wüthrich, *J. Am. Chem. Soc.* **1988**, *110*, 2388 – 2393.
[4] J. E. Coleman, *Methods Enzymol.* **1993**, *227*, 16 – 43.
[5] C. J. Henehan, D. L. Pountney, O. Zerbe, M. Vasak, *Protein Sci.* **1993**, *2*, 1756 – 1764.
[6] G. L. Oz, D. L. Pountney, I. M. Armitage, *Biochem. Cell Biol.* **1998**, *76*, 223 – 234.
[7] L. M. Utschig, J. G. Wright, G. Dieckmann, V. L. Pecoraro, T. V. O'Halloran, *Inorg. Chem.* **1995**, *34*, 2497 – 2498.
[8] L. M. Utschig, T. Abynard, C. Strong, T. V. O'Halloran, *Inorg. Chem.* **1997**, *36*, 2926 – 2927.
[9] O. Zerbe, D. L. Pountney, W. von Philipsborn, M. Vasak, *J. Am. Chem. Soc.* **1994**, *116*, 377 – 378.
[10] F. Arnesano, L. Banci, I. Bertini, S. Mangani, A. R. Thompsett, *Proc. Natl. Acad. Sci. USA* **2003**, *100*, 3814 – 3819.
[11] L. Banci, I. Bertini, F. Cantini, S. Ciofi-Baffoni, L. Gonnelli, S. Mangani, *J. Biol. Chem.* **2005**, *279*, 34833 – 34839.
[12] J. E. Penner-Hahn, *Coord. Chem. Rev.* **1999**, *190–192*, 1101 – 1123.
[13] L. Banci, I. Bertini, S. Mangani, *J. Synchrotron Rad.* **2005**, *12*, 94 – 97.
[14] F. A. Walker in *The Porphyrin Handbook, Vol. 5*, (Eds.: K. M. Kadish, K. M. Smith, R. Guilard), Academic Press, San Diego, CA, **2000**, pp. 81 – 183.
[15] M. Ubbink, J. A. R. Worrall, G. W. Canters, E. J. J. Groenen, M. Huber, *Annu. Rev. Biophys. Biomol. Struct.* **2002**, *31*, 393 – 422.
[16] A. Abragam, B. Bleaney, *Electron Paramagnetic Resonance of Transition Metal Ions*, Clarendon Press, Oxford, **1970**.
[17] C. P. Slichter, *Principles of Magnetic Resonance*, 1st ed., Springer, Berlin, **1989**.
[18] R. Kubo, K. Tomita, *J. Phys. Soc. Jpn* **1954**, *9*, 888 – 919.
[19] I. Solomon, *Phys. Rev.* **1955**, *99*, 559 – 565.
[20] M. Gueron, *J. Magn. Reson.* **1975**, *19*, 58 – 66.
[21] A. J. Vega, D. Fiat, *Mol. Phys.* **1976**, *31*, 347 – 355.
[22] M. Allegrozzi, I. Bertini, M. B. L. Janik, Y.-M. Lee, G. Liu, C. Luchinat, *J. Am. Chem. Soc.* **2000**, *122*, 4154 – 4161.
[23] I. Bertini, A. Donaire, B. Jiménez, C. Luchinat, G. Parigi, M. Piccioli, L. Poggi, *J. Biomol. NMR* **2001**, *21*, 85 – 98.
[24] L. W. Donaldson, N. R. Skrynnikov, W.-Y. Choy, D. R. Muhandiram, B. Sarkar, J. D. Forman-Kay, L. E. Kay, *J. Am. Chem. Soc.* **2001**, *123*, 9843 – 9847.
[25] V. Gaponenko, A. S. Altieri, J. Li, R. A. Byrd, *J. Biomol. NMR* **2002**, *24*, 143 – 148.
[26] I. Bertini, I. Gelis, N. Katsaros, C. Luchinat, A. Provenzani, *Biochemistry* **2003**, *42*, 8011 – 8021.
[27] J. Wöhnert, K. J. Franz, M. Nitz, B. Imperiali, H. Schwalbe, *J. Am. Chem. Soc.* **2003**, *125*, 13338 – 13339.
[28] I. Baig, I. Bertini, C. Del Bianco, Y. K. Gupta, Y.-M. Lee, C. Luchinat, A. Quattrone, *Biochemistry* **2004**, *43*, 5562 – 5573.
[29] I. Bertini, M. Fragai, Y.-M. Lee, C. Luchinat, B. Terni, *Angew. Chem.* **2004**, *116*, 2304 – 2306; *Angew. Chem. Int. Ed.* **2004**, *43*, 2254 – 2256.
[30] V. Gaponenko, S. P. Sarma, A. S. Altieri, D. A. Horita, J. Li, R. A. Byrd, *J. Biomol. NMR* **2004**, *28*, 205 – 212.
[31] T. Ikegami, L. Verdier, P. Sakhaii, S. Grimme, P. Pescatore, K. Saxena, K. M. Fiebig, C. Griesinger, *J. Biomol. NMR* **2004**, *29*, 339 – 349.
[32] M. Prudencio, J. Rohovec, J. A. Peters, E. Tocheva, M. J. Boulanger, M. E. Murphy, H. J. Hupkes, W. Koster, A. Impagliazzo, M. Ubbink, *Chem. Eur. J.* **2004**, *10*, 3252 – 3260.
[33] M. R. Jensen, C. Lauritzen, S. W. Dahl, J. Pedersen, J. J. Led, *J. Biomol. NMR* **2004**, *29*, 175 – 185.
[34] V. Gaponenko, A. Dvoretsky, C. Walsby, B. M. Hoffman, P. R. Rosevear, *Biochemistry* **2000**, *39*, 15217 – 15224.
[35] G. Pintacuda, A. Moshref, A. Leonchiks, A. Sharipo, G. Otting, *J. Biomol. NMR* **2004**, *29*, 351 – 361.
[36] D. L. Turner, *Eur. J. Biochem.* **1993**, *211*, 563 – 568.
[37] I. Bertini, F. Capozzi, C. Luchinat, M. Piccioli, A. J. Vila, *J. Am. Chem. Soc.* **1994**, *116*, 651 – 660.
[38] D. L. Turner, C. A. Salgueiro, P. Schenkels, J. LeGall, A. V. Xavier, *Biochim. Biophys. Acta* **1995**, *1246*, 24 – 28.
[39] L. Banci, R. Pierattelli, D. L. Turner, *Eur. J. Biochem.* **1995**, *232*, 522 – 527.
[40] N. V. Shokhirev, F. A. Walker, *J. Phys. Chem.* **1995**, *99*, 17795 – 17804.
[41] I. Bertini, A. Donaire, B. A. Feinberg, C. Luchinat, M. Piccioli, H. Yuan, *Eur. J. Biochem.* **1995**, *232*, 192 – 205.
[42] R. Pierattelli, L. Banci, D. L. Turner, *J. Biol. Inorg. Chem.* **1996**, *1*, 320 – 329.
[43] R. Pierattelli, D. L. Turner, *Eur. Biophys. J.* **1996**, *24*, 342 – 347.
[44] I. Bertini, A. Dikiy, C. Luchinat, R. Macinai, M. S. Viezzoli, *Inorg. Chem.* **1998**, *37*, 4814 – 4821.
[45] S. Aono, D. Bentrop, I. Bertini, A. Donaire, C. Luchinat, Y. Niikura, A. Rosato, *Biochemistry* **1998**, *37*, 9812 – 9826.
[46] S. J. Wilkens, B. Xia, F. Weinhold, J. L. Markley, W. M. Westler, *J. Am. Chem. Soc.* **1998**, *120*, 4806 – 4814.
[47] N. V. Shokhirev, F. A. Walker, *J. Biol. Inorg. Chem.* **1998**, *3*, 581 – 594.
[48] I. Bertini, C. Luchinat, G. Parigi, F. A. Walker, *J. Biol. Inorg. Chem.* **1999**, *4*, 515 – 519.
[49] I. Bertini, S. Ciurli, A. Dikiy, R. Gasanov, C. Luchinat, G. Martini, N. Safarov, *J. Am. Chem. Soc.* **1999**, *121*, 2037 – 2046.
[50] I. Bertini, C. O. Fernández, B. G. Karlsson, J. Leckner, C. Luchinat, B. G. Malmström, A. M. Nersissian, R. Pierattelli, E. Shipp, J. S. Valentine, A. J. Vila, *J. Am. Chem. Soc.* **2000**, *122*, 3701 – 3707.
[51] L. Banci, I. Bertini, G. Cavallaro, C. Luchinat, *J. Biol. Inorg. Chem.* **2002**, *7*, 416 – 426.
[52] T. E. Machonkin, W. M. Westler, J. L. Markley, *J. Am. Chem. Soc.* **2004**, *126*, 5413 – 5426.

[53] T. E. Machonkin, W. M. Westler, J. L. Markley, *Inorg. Chem.* **2005**, *44*, 779 – 797.
[54] C. A. Salgueiro, D. L. Turner, A. V. Xavier, *Eur. J. Biochem.* **1997**, *244*, 721 – 734.
[55] B. Xia, W. M. Westler, H. Cheng, J. Meyer, J.-M. Moulis, J. L. Markley, *J. Am. Chem. Soc.* **1995**, *117*, 5347 – 5350.
[56] I. Bertini, Y.-M. Lee, C. Luchinat, M. Piccioli, L. Poggi, *ChemBioChem* **2001**, *2*, 550 – 558.
[57] H. M. McConnell, R. E. Robertson, *J. Chem. Phys.* **1958**, *29*, 1361 – 1365.
[58] M. Gochin, H. Roder, *Bull. Magn. Reson.* **1995**, *17*, 1 – 4.
[59] I. Bertini, C. Luchinat, G. Parigi, *Progr. NMR Spectrosc.* **2002**, *40*, 249 – 273.
[60] M. Gochin, H. Roder, *Protein Sci.* **1995**, *4*, 296 – 305.
[61] L. Banci, I. Bertini, K. L. Bren, M. A. Cremonini, H. B. Gray, C. Luchinat, P. Turano, *J. Biol. Inorg. Chem.* **1996**, *1*, 117 – 126.
[62] D. L. Turner, L. Brennan, S. G. Chamberlin, R. O. Louro, A. V. Xavier, *Eur. Biophys. J.* **1998**, *27*, 367 – 375.
[63] I. Bertini, C. Luchinat, G. Parigi, *Concepts Magn. Reson.* **2002**, *14*, 259 – 286.
[64] R. Barbieri, C. Luchinat, G. Parigi, *ChemPhysChem* **2004**, *5*, 797 – 806.
[65] L. Banci, I. Bertini, G. Cavallaro, A. Giachetti, C. Luchinat, G. Parigi, *J. Biomol. NMR* **2004**, *28*, 249 – 261.
[66] I. Bertini, C. Luchinat, G. Parigi, *Eur. J. Inorg. Chem.* **2000**, 2473 – 2480.
[67] G. Williams, N. J. Clayden, G. R. Moore, R. J. P. Williams, *J. Mol. Biol.* **1985**, *183*, 447 – 460.
[68] B. D. Nguyen, Z. Xia, D. C. Yeh, K. Vyas, H. Deaguero, G. N. La Mar, *J. Am. Chem. Soc.* **1999**, *121*, 208 – 217.
[69] Z. Xia, B. D. Nguyen, G. N. La Mar, *J. Biomol. NMR* **2000**, *17*, 167 – 174.
[70] L. Lee, B. D. Sykes, *Biochemistry* **1983**, *22*, 4366 – 4373.
[71] L. Banci, I. Bertini, M. A. Cremonini, G. Gori Savellini, C. Luchinat, K. Wüthrich, P. Güntert, *J. Biomol. NMR* **1998**, *12*, 553 – 557.
[72] K. Tu, M. Gochin, *J. Am. Chem. Soc.* **1999**, *121*, 9276 – 9285.
[73] L. Brennan, D. L. Turner, A. C. Messias, M. L. Teodoro, J. LeGall, H. Santos, A. V. Xavier, *J. Mol. Biol.* **2000**, *298*, 61 – 82.
[74] K. L. Bren, J. A. Kellogg, R. Kaur, X. Wen, *Inorg. Chem.* **2004**, *43*, 7934 – 7944.
[75] B. J. Goodfellow, S. G. Nunes, F. Rusnak, I. Moura, C. Ascenso, J. J. Moura, B. F. Volkman, J. L. Markley, *Protein Sci.* **2002**, *11*, 2464 – 2470.
[76] L. Banci, I. Bertini, G. Gori Savellini, A. Romagnoli, P. Turano, M. A. Cremonini, C. Luchinat, H. B. Gray, *Proteins Struct. Funct. Genet.* **1997**, *29*, 68 – 76.
[77] D. A. Case, D. A. Pearlman, J. W. Caldwell, T. E. Cheatham, W. S. Ross, C. L. Simmerling, T. A. Darden, K. M. Merz, R. V. Stanton, A. L. Cheng, J. J. Vincent, M. Crowley, V. Tsui, R. J. Radmer, Y. Duan, J. Pitera, I. Massova, G. L. Seibel, U. C. Singh, P. K. Weiner, P. A. Kollman, *AMBER 6*, University of California, San Francisco, **1999**.
[78] G. Pintacuda, M. A. Keniry, T. Huber, A. Y. Park, N. E. Dixon, G. Otting, *J. Am. Chem. Soc.* **2004**, *126*, 2963 – 2970.
[79] R. D. Guiles, S. Sarma, R. J. DiGate, D. Banville, V. J. Basus, I. D. Kuntz, L. Waskell, *Nat. Struct. Biol.* **1996**, *3*, 333 – 339.
[80] D. L. Turner, R. J. P. Williams, *Eur. J. Biochem.* **1993**, *211*, 555 – 562.
[81] N. U. Jain, T. C. Pochapsky, *J. Am. Chem. Soc.* **1998**, *120*, 12984 – 12985.
[82] B. Xia, B. F. Volkman, J. L. Markley, *Biochemistry* **1998**, *37*, 3965 – 3973.
[83] D. Zhao, H. M. Hutton, P. R. Gooley, N. E. MacKenzie, M. Cusanovich, *Protein Sci.* **2000**, *9*, 1828 – 1837.
[84] I. Bertini, C. Luchinat, P. Turano, *J. Biol. Inorg. Chem.* **2000**, *5*, 761 – 764.
[85] I. Bertini, C. Luchinat, G. Parigi, *Solution NMR of Paramagnetic Molecules*, Elsevier, Amsterdam, **2001**.
[86] I. Bertini, A. Donaire, C. Luchinat, A. Rosato, *Proteins Struct. Funct. Genet.* **1997**, *29*, 348 – 358.
[87] S. U. Dunham, C. J. Turner, S. J. Lippard, *J. Am. Chem. Soc.* **1998**, *120*, 5395 – 5406.
[88] A. Ramos, G. Varani, *J. Am. Chem. Soc.* **1998**, *120*, 10992 – 10993.
[89] J. Kowalewski, C. Luchinat, T. Nilsson, G. Parigi, *J. Phys. Chem. A* **2002**, *106*, 7376 – 7382.
[90] I. Bertini, G. Cavallaro, M. Cosenza, R. Kummerle, C. Luchinat, M. Piccioli, L. Poggi, *J. Biomol. NMR* **2002**, *23*, 115 – 125.
[91] I. Bertini, C. Luchinat, D. Tarchi, *Chem. Phys. Lett.* **1993**, *203*, 445 – 449.
[92] I. Bertini, C. Luchinat, M. Piccioli, D. Tarchi, *Concepts Magn. Reson.* **1994**, *6*, 307 – 335.
[93] J. Boisbouvier, P. Gans, M. Blackledge, B. Brutscher, D. Marion, *J. Am. Chem. Soc.* **1999**, *121*, 7700 – 7701.
[94] J. C. Hus, D. Marion, M. Blackledge, *J. Mol. Biol.* **2000**, *298*, 927 – 936.
[95] P. K. Madhu, P. K. Mandal, N. Muller, *J. Magn. Reson.* **2002**, *155*, 29 – 38.
[96] G. Pintacuda, K. Hohenthanner, G. Otting, N. Muller, *J. Biomol. NMR* **2003**, *27*, 115 – 132.
[97] P. Turano, G. Battaini, L. Casella, *Chem. Phys. Lett.* **2003**, *373*, 460 – 463.
[98] G. Pintacuda, A. Kaikkonen, G. Otting, *J. Magn. Reson.* **2004**, *171*, 233 – 243.
[99] N. Tjandra, A. Bax, *Science* **1997**, *278*, 1111 – 1114.
[100] J. R. Tolman, J. M. Flanagan, M. A. Kennedy, J. H. Prestegard, *Proc. Natl. Acad. Sci. USA* **1995**, *92*, 9279 – 9283.
[101] L. Banci, I. Bertini, J. G. Huber, C. Luchinat, A. Rosato, *J. Am. Chem. Soc.* **1998**, *120*, 12903 – 12909.
[102] J. R. Tolman, J. M. Flanagan, M. A. Kennedy, J. H. Prestegard, *Nat. Struct. Biol.* **1997**, *4*, 292 – 297.
[103] A. Bax, N. Tjandra, *Nat. Struct. Biol.* **1997**, *4*, 254 – 256.
[104] A. A. Bothner-By, J. P. Domaille, C. Gayathri, *J. Am. Chem. Soc.* **1981**, *103*, 5602 – 5603.
[105] W. Peti, J. Meiler, R. Brüschweiler, C. Griesinger, *J. Am. Chem. Soc.* **2002**, *124*, 5822 – 5833.
[106] J. R. Tolman, *J. Am. Chem. Soc.* **2002**, *124*, 12020 – 12030.
[107] J. C. Hus, D. Marion, M. Blackledge, *J. Am. Chem. Soc.* **2001**, *123*, 1541 – 1542.
[108] I. Bertini, M. Longinetti, C. Luchinat, G. Parigi, L. Sgheri, *J. Biomol. NMR* **2002**, *22*, 123 – 136.
[109] R. Barbieri, I. Bertini, G. Cavallaro, Y.-M. Lee, C. Luchinat, A. Rosato, *J. Am. Chem. Soc.* **2002**, *124*, 5581 – 5587.
[110] I. Bertini, M. B. L. Janik, G. Liu, C. Luchinat, A. Rosato, *J. Magn. Reson.* **2001**, *148*, 23 – 30.
[111] I. Bertini, M. B. L. Janik, Y.-M. Lee, C. Luchinat, A. Rosato, *J. Am. Chem. Soc.* **2001**, *123*, 4181 – 4188.
[112] I. Bertini, C. Del Bianco, I. Gelis, N. Katsaros, C. Luchinat, G. Parigi, M. Peana, A. Provenzani, M. A. Zoroddu, *Proc. Natl. Acad. Sci. USA* **2004**, *101*, 6841 – 6846.
[113] Z. Serber, C. Richter, D. Moskau, J.-M. Boehlen, T. Gerfin, D. Marek, M. Haeberli, L. Baselgia, F. Laukien, A. S. Stern, J. C. Hoch, V. Doetsch, *J. Am. Chem. Soc.* **2000**, *122*, 3554 – 3555.
[114] U. Kolczak, J. Salgado, G. Siegal, M. Saraste, G. W. Canters, *Biospectroscopy* **1999**, *5*, S19-S32.
[115] T. E. Machonkin, W. M. Westler, J. L. Markley, *J. Am. Chem. Soc.* **2002**, *124*, 3204 – 3205.
[116] T. C. Pochapsky, S. S. Pochapsky, T. Ju, H. Mo, F. Al-Mjeni, M. J. Maroney, *Nat. Struct. Biol.* **2002**, *9*, 966 – 972.
[117] M. Kostic, S. S. Pochapsky, T. C. Pochapsky, *J. Am. Chem. Soc.* **2002**, *124*, 9054 – 9055.
[118] W. Bermel, I. Bertini, I. C. Felli, R. Kummerle, R. Pierattelli, *J. Am. Chem. Soc.* **2003**, *125*, 16423 – 16429.
[119] E. Babini, I. Bertini, F. Capozzi, I. C. Felli, M. Lelli, C. Luchinat, *J. Am. Chem. Soc.* **2004**, *126*, 10496 – 10497.
[120] I. Bertini, B. Jiménez, M. Piccioli, *J. Magn. Reson.* **2005**, *174*, 125 – 132.
[121] I. Bertini, L. Duma, I. C. Felli, M. Fey, C. Luchinat, R. Pierattelli, P. Vasos, *Angew. Chem.* **2004**, *116*, 2307 – 2309; *Angew. Chem. Int. Ed.* **2004**, *43*, 2257 – 2259.
[122] W. Bermel, I. Bertini, I. C. Felli, R. Pierattelli, P. R. Vasos, *J. Magn. Reson.* **2005**, *172*, 324 – 328.
[123] F. Arnesano, L. Banci, I. Bertini, I. C. Felli, C. Luchinat, A. R. Thompsett, *J. Am. Chem. Soc.* **2003**, *125*, 7200 – 7208.
[124] G. Vogeli, H. Kovacs, K. Pervushin, *J. Biomol. NMR* **2005**, *31*, 1 – 9.
[125] M. Ottiger, F. Delaglio, A. Bax, *J. Magn. Reson.* **1998**, *131*, 373 – 378.
[126] P. Andersson, J. Weigelt, G. Otting, *J. Biomol. NMR* **1998**, *12*, 435 – 441.
[127] L. Duma, S. Hediger, B. Brutscher, A. Bockmann, L. Emsley, *J. Am. Chem. Soc.* **2003**, *125*, 11816 – 11817.
[128] W. Bermel, I. Bertini, L. Duma, L. Emsley, I. C. Felli, R. Pierattelli, P. Vasos, *Angew. Chem.* **2005**, *117*, 3149 – 3152; *Angew. Chem. Int. Ed.* **2005**, *44*, 3089 – 3092.
[129] N. C. Nielsen, H. Thøgersen, O. W. Sørensen, *J. .Am. Chem. Soc.* **1995**, *117*, 11365 – 11366.
[130] E. Babini, I. Bertini, F. Capozzi, C. Del Bianco, D. Holleder, T. Kiss, C. Luchinat, A. Quattrone, *Biochemistry* **2004**, *43*, 16076 – 16085.

[131] L. E. Kay, P. Keifer, T. Saarinen, *J. Am. Chem. Soc.* **1992**, *114*, 10663 – 10665.
[132] M. P. Williamson, T. F. Havel, K. Wüthrich, *J. Mol. Biol.* **1985**, *185*, 295 – 315.
[133] G. Wagner, *Progr. NMR Spectrosc.* **1990**, *22*, 101 – 139.
[134] G. N. La Mar, F. A. Walker in *The Porphyrins* (Ed.: D. Dolphin), Academic Press, New York, **1979**, pp. 61 – 157.
[135] B.-H. Oh, J. L. Markley, *Biochemistry* **1990**, *29*, 4012 – 4017.
[136] S. C. Busse, G. N. La Mar, J. B. Howard, *J. Biol. Chem.* **1991**, *266*, 23714 – 23723.
[137] J. S. de Ropp, G. N. La Mar, *J. Am. Chem. Soc.* **1991**, *113*, 4348 – 4350.
[138] J. Gaillard, J.-P. Albrand, J.-M. Moulis, D. E. Wemmer, *Biochemistry* **1992**, *31*, 5632 – 5639.
[139] M. Sette, J. S. de Ropp, G. Hernandez, G. N. La Mar, *J. Am. Chem. Soc.* **1993**, *115*, 5237 – 5245.
[140] F. A. Walker, U. Simonis in *NMR of Paramagnetic Molecules* (Eds.: L. J. Berliner, J. Reuben), Plenum, New York, **1993**, pp. 133 – 274.
[141] J. D. Satterlee, S. Alam, Q. Yi, J. E. Erman, I. Constantinidis, D. J. Russel, S. J. Moench in *Biological Magnetic Resonance, Vol.* 12 (Eds.: L. J. Berliner, J. Reuben), Plenum, New York, **1993**, pp. 275 – 298.
[142] D. L. Turner, *J. Magn. Reson. Ser. A* **1993**, *104*, 197 – 202.
[143] L. Banci, *Biol. Magn. Reson.* **1993**, *12*, 79 – 111.
[144] L. Banci, I. Bertini, L. D. Eltis, I. C. Felli, D. H. W. Kastrau, C. Luchinat, M. Piccioli, R. Pierattelli, M. Smith, *Eur. J. Biochem.* **1994**, *225*, 715 – 725.
[145] I. Bertini, C. Luchinat, M. Piccioli, *Methods Enzymol.* **2001**, *339*, 314 – 340.
[146] I. Bertini, C. Luchinat, G. Parigi, *Adv. Inorg. Chem.* **2005**, *57*, 105.

Received: March 29, 2005
Published online on August 11, 2005

